Transport Capacity of Opportunistic Spectrum Access (OSA) MANETs

(Invited Paper)

Cesar Santivanez (csantiva@bbn.com)
BBN Technologies, Cambridge, MA 02138

***Abstract*—In this paper, we study the Transport Capacity (TC) of a Mobile Ad hoc NETwork (MANET) of secondary nodes without a predefined bandwidth assignment. These secondary users' access of the spectrum is governed by Opportunistic Spectrum Access (OSA) rules, i.e., they can use portions of the spectrum as long as their transmissions do not interfere with the spectrum's primary (protected) users.**

We present an analytical framework to compute the TC (bits-meter per second) of OSA MANETs. Our results show that an OSA MANET exhibits two operating regions, determined by the ratio of the secondary nodes' transmission range (l_s) over the primary nodes' (l_p). When $l_s < l_p$, the OSA MANET is in the *interference limited* region, and its TC behaves exactly as a *legacy* MANET, that is, its TC decays slowly with respect to l_s: $TC \approx k\frac{A\,W}{l_s} = \Theta\left(l_s^{-1}\right)$, where A is the network area, and W is the usable spectrum. However, when $l_s > l_p$, the OSA MANET is in the *policy limited* region, where TC decays faster than before w.r.t. l_s, that is, $TC \approx k'\frac{A\,W}{l_s}\left(\frac{l_p}{l_s}\right)^{\alpha-2} = \Theta\left(l_s^{-(\alpha-1)}\right)$ if density is unbounded, and $TC \approx k''\frac{A\,W}{l_s}\left(\frac{l_p}{l_s}\right)^{\alpha} = \Theta\left(l_s^{-(\alpha+1)}\right)$ if density is bounded, where $\alpha > 2$ is the pathloss exponent.

These results are of great importance to understand the behavior of OSA-enabled MANETs, especially when designing a network (e.g., number of nodes, density, needed to cover an area) or developing self-optimizing algorithms (e.g., topology control).

I. Introduction

Traditional rigid spectrum access rules are believed to be the main cause of the (apparent) spectrum scarcity problem. Opportunistic Spectrum Access (OSA) has recently emerged as a potential solution. Under OSA, nodes are allowed to access a particular frequency band as long as their transmissions do not cause harmful interference to the primary (protected) users of that band.[1], [2]. OSA represents a new paradigm for Mobile Ad hoc NETworks (MANETs) and as such it challenges our current understanding of MANET tradeoffs, behaviors, and scaling laws. Currently, there is a lack of fundamental results on OSA MANET's behavior.

In this paper we consider a scenario where two set of nodes coexist in the same physical area: a network of *primary* nodes, with protected usage rights over the usable spectrum W, and a set of OSA-enabled secondary nodes (referred to as OSA MANET), which do not have any preassigned frequency band, but access the spectrum following OSA rules. We answer a fundamental question: how is the Transport Capacity (TC) [3] of an OSA MANET different from that of a *legacy* MANET.[1] We study the TC, defined in this paper as the number of bits simultaneously transmitted per unit of time, times the distance these bits travel. This bandwidth-distance definition of TC is slightly different than the one typically used in the literature, which considers end-to-end flows as opposed to single-hop transmissions. However, both quantities are directly related and asymptotically equivalent[2]. The TC defined above is much simpler to compute and provides a very good indicator of a network's ability to satisfy the upper layer's communication requirements when the exact nature/patterns of these requirements are not known in advance. For example, if the number of nodes is N and the average source-destination distance is L, then the per node end-to-end (i.e., multi-hop) throughput is roughly $\Theta(\frac{TC}{N\,L})$.

We start by providing an analytical framework to compute TC. We then use this framework to determine whether previously reported behavior[15] (i.e., TC's fast decay when the transmission range of the secondary nodes exceeds that of the primary nodes) followed a fundamental limitation of OSA MANETs, or was technology-dependent.

Initially we assume that the density of the secondary nodes is unbounded, and the control parameter is the secondary nodes' transmission range l_s. This setting is useful when designing topology-control algorithms. We consider three modulation models: *Full-rate*, *Semilinear*, and *Shannon*. The *Full-rate* model is the closest to the one employed [15]. The *Shannon* model corresponds to the theoretically best possible modulation (assuming infinite delays are tolerable). The *Semi-linear* model is in-between: it is practically implementable

Research was sponsored by the U.S. Army Research Laboratory and the U.K. Ministry of Defence and was accomplished under Agreement Number W911NF-06-3-0001. The views and conclusions contained in this document are those of the author(s) and should not be interpreted as representing the official policies, either expressed or implied, of the U.S. Army Research Laboratory, the U.S. Government, the U.K. Ministry of Defence or the U.K. Government. The U.S. and U.K. Governments are authorized to reproduce and distribute reprints for Government purposes notwithstanding any copyright notation hereon.

[1]The term *legacy* MANET refers to a "classical" MANET where the nodes are assigned exclusive access to the frequency spectrum and have no limit — other than hardware limitations — on their transmission power. *Legacy* MANETs are used as a benchmark against OSA MANETs, which have additional transmission power constraint and therefore exhibit lower performance. However, it should be kept in mind that OSA MANETs can operate in spectrum bands where *legacy* MANETs simply cannot.

[2]The work in [3] shows that, for uniformly distributed networks, the main limit on capacity is not the formation of hot-spots in the center of the network but "the pervasive need for all nodes to share the channel locally with other nodes."

(and analytically tractable) and — within an order of magnitude — tracks the performance of the *Shannon* model. Our results show that while the steep decay observed in the [15] and the *Full rate* models are dominated by their modulation schemes' inability to exploit opportunities with small SINR — and it is therefore technology dependent, — OSA MANETs present two operating regions, regardless of the modulation scheme being used. When the transmission range (l_s) of the secondary nodes is small compared to the primary nodes' (l_p) the OSA MANET is in the *interference limited* region, where TC varies slowly with respect to l_s (i.e., $TC = \Theta\left(\frac{1}{l_s}\right)$), as in *legacy* MANETs. However, when the transmission range of the secondary nodes is larger than the primary nodes', the OSA MANET is in the *policy limited* region. When in the *policy limited* region, high data rate transmissions are not possible, large processing gains (or equivalent) are needed, and the $TC = \Theta\left(e^{-k\left(\frac{l_s}{l_p}\right)^2}\right)$ for the *Full rate* model, and $TC = \Theta\left(\frac{1}{l_s}\left(\frac{l_p}{l_s}\right)^{\alpha-2}\right)$ for the *Semilinear* and *Shannon* models.

We then shift our attention to the topology design problem (e.g., dimensioning the network) where the control parameter is the (bounded) density (or equivalently, the number) of secondary nodes. It is assumed that the secondary nodes use the optimal (i.e., smallest) transmission range that keeps the network connected([3], [16]). We observe that while we still have two operating regions, the same transition point, and the same behavior in the *interference-limited* region, the rate of decay in the *policy-limited* region is faster than before — i.e., $TC = \Theta\left(\frac{1}{l_s}\left(\frac{l_p}{l_s}\right)^{\alpha}\right)$ for the *Semilinear* and *Shannon* models. These results, showing the fundamental difference between OSA and *legacy* MANETs, provide designers with great insight into the network's tradeoffs. For example, in a *legacy* MANET of N nodes we require $3N$ relay nodes to double the TC. But in an OSA MANET operating in the *policy limited* region (and assuming $\alpha = 4$), the number of relay nodes required is just $0.32N$ (i.e., 10 times lower). Therefore, the use of relay nodes is much more attractive for OSA MANETs operating in the *policy limited* region.

The remainder of this paper is organized as follows. The next section discusses the previous work. Section III presents our framework to compute the TC for an OSA MANET. Section IV applies the framework to three broad classes of modulation schemes, for the unbounded density case. Section V extends the previous analysis for the case of bounded density. Finally, Section VI summarizes our results.

II. Related Work

Since the seminal work in [3], the TC for *legacy* MANETs has been the subject of much study (e.g., [4], [5]). These results, however, are not directly applicable to OSA MANETs.

OSA MANETs have been the subject of recent attention. In 2002, DARPA launched its XG program, with the goal to develop both the enabling technologies and system concepts for OSA[6]. However, most works addressing OSA MANETs to date (e.g., [7]–[10]), have limited their focus to particular algorithms, such as channel selection or MAC protocols.

From the few works addressing system-wide issues for OSA MANETs (e.g., [11]–[15]), only our work in [15] reports results on the OSA MANET's capacity and its dependence on the secondary nodes' transmission range. [15] observes that the capacity in an OSA MANET decays much faster than in *legacy* MANETs with respect to the transmission range, and therefore stresses the importance of a topology control module for OSA MANETs. However, the study in [15] is simulation-based and its results are technology dependent, which limits the scope of its applicability.

In this paper, we present an analytical framework that explains our results in [15], generalizes them, and shows that while the observed steep decay of the TC is an artifact of the particular technology used, the existence of a *policy-limited* region — where the TC decays faster than in *legacy* MANETs — is a fundamental property of OSA MANETs.

III. A Framework to compute TC

We study a MANET of secondary users coexisting with a network of primary users in a large flat area A. The usable spectrum W is divided into M equal bands $f_1, f_2, \cdots, f_M$, each experiencing a background noise η_0. Each band is assigned to a class of primary users. That is, primary users of class m have protected usage rights over frequency band f_m and can freely transmit over this band. A secondary user may access any band or combination thereof, as long as the interference induced over *any* primary node is below that node's interference tolerance η_p. Thus, the effect of the presence of a primary node in the vicinity of a secondary node is to limit the transmission power of the latter to a value P_m dependent on the distance between the secondary and its closest primary node. Since the primary nodes' position is a random variable, so is the secondary nodes' allowed transmission power. We denote by $f_P()$ the probability density function (pdf) of the secondary nodes' allowed transmission power due to the primary network. To facilitate and ground the analysis we assume that:

1) Single-user reception per-band: Secondary nodes have multi-user communication capabilities that allow them to simultaneously decode — at each band – the transmissions from the primary nodes[3] as well as one (and only one) of the transmissions from the secondary nodes. Signals from other secondary nodes are treated as noise. Thus, secondary nodes can resolve interference from primary nodes, and simultaneously decode multiple packets from different secondary nodes,

[3]This assumption may be too optimistic since it may not be possible to resolve the primary node' signals in all the situations. In particular, weak primary signals may not be distinguishable from noise. However, in those situations the secondary signals' will be the main contributor to interference so that our ignoring the primary signals when computing interference will have little impact. Similarly, we are assuming that perfect reconstruction/removal of primary signals is possible, while in practice a small amount of residual error is unavoidable. We ignore these issues to obtain a theoretical technology-independent (tight) upper bound.

as long as these packets arrive over different (orthogonal) frequency bands.

Note that the main difference between primary and secondary nodes' signals is that the former typically have well known, predictable waveforms and MAC timing (e.g., a GSM base station), while the latter may continuously change (i.e., morph) their waveform and MAC timing to adapt to current opportunities and traffic loads (OSA MANETs). Thus, synchronization and multi-user reception are more easily done with primary node's signals than with the highly dynamic signals from secondary nodes.

2) Frequency bands' independence: Each frequency band can be independently accessed by each secondary node.

This implies that the same secondary node can transmit in a frequency band while it is receiving a packet in another. While this is hard to achieve with today's hardware — the high power from the transmission circuitry spills over (as noise) into the reception circuitry — this assumption is made to allow for a simple, tractable model that within reason approximates the TC. Besides, we can always rearrange the set of transmitters and receivers to obtain another set with similar total TC where the same node does not transmit and receive at the same time.

3) Physical layer model: The power attenuation between a transmitter i and a receiver j is a polynomial function of their Euclidean distance d_{ij}. Specifically, when node i transmits with power P, node j receives a signal of power $\frac{P}{\kappa d_{ij}^{\alpha}}$, where $\alpha > 2$ is referred to as the *pathloss exponent*.[4]

Note that κ is a constant that takes into account the carrier signal's wavelength, and the antenna gain. Since the usable spectrum W is typically narrow compared with its center frequency, the carrier wavelengths corresponding to the bands $f_1, f_2, \cdots, f_M$ are all very similar and can be approximated with a single value. The node's antennas are assumed to be azimuthally isotropic, and therefore their gain is the same in all directions. This assumption is made for simplicity and clarity, and our model can be easily extended to accommodate directional antennas, with little impact on our results.

4) Primary nodes: Primary nodes of class m are uniformly distributed in area A with a density σ_p and have a transmission range l_p. These nodes have a target Signal-to-Noise Ratio (SNR) of θ_p, that is, for nodes at a distance l_p, the received signal strength must be at least $\theta_p\, \eta_0$.

5) Secondary nodes: Secondary nodes are also uniformly distributed in the area A with a density σ_s and have a transmission range l_s. The rest of the parameters of secondary nodes are dynamically adjusted to optimize the network's TC. For simplicity, we assume that there is no physical limitation on the transmission power.

[4]We consider values of α strictly greater than 2 since for large networks, a value of $\alpha = 2$ is not realistic, and results in a cumulative interference that doesn't converge to a bounded value but continuously increases with the network area. Also, technically the above expression is valid only for d_{ij} greater than a frequency-specific reference distance and $\kappa^{\frac{1}{\alpha}}$. We relax these constraints for simplicity in the analysis, and because they have no impact in our results for practical scenarios – where both the transmission distances l_s as well as the resulting optimal spatial reuse distances are within the valid region of the above pathloss expression.

6) Spatial reuse: A node may reuse a band used by other nodes in its network, as long as its distance to any other node currently transmitting or receiving is greater than a configurable minimum distance referred to as the *spatial reuse distance* (τ). For secondary nodes, *spatial reuse distance* τ is a controllable parameter. For primary nodes, we assume that their spatial reuse distance τ_p is fixed and equal to the nodes' carrier sensing range, i.e., $\tau_p = \theta_p^{\frac{1}{\alpha}} l_p$.

For a given value of τ, the expected number of simultaneous transmitters (N_{Active}) in a network of area A is equal to $N_{Active} = \frac{A h_\tau}{\pi \tau^2}$. While in general h_τ depends on τ, it varies slowly (e.g., h_τ just doubles when τ varies from 0 to infinity), and therefore we consider it to be fixed and equal to h_p and h_s for primary and secondary nodes, respectively.

While imposing a minimum distance from a transmitter to any receiver is obvious and mandatory (to limit the amount of interference a single transmitter may induce into a receiver), imposing a minimum distance to other transmitters is not. This minimum distance is required to limit the number of closely located transmitters, and so to prevent that their combined transmission power adds up to a huge interference level at a close-by receiver. However, it should be noted that this is not the only way to control the cumulative interference. This method was chosen due to its simplicity (i.e., it is basically *carrier sensing*) and because it allows for a quick derivation of the number of simultaneous transmitters. Further, it does not result in loss of generality, since its effect in the analysis is to relate the interference level ($I = \Theta\left(\frac{P}{\tau^\alpha}\right)$) to the number of simultaneous transmitters ($N_{Active} = \Theta\left(\frac{A}{\tau^2}\right)$) in a fairly general and sensible way (i.e., $I = \Theta\left(\left(\frac{N_{Active}}{A}\right)^{\frac{\alpha}{2}} P\right)$.

Table I summarizes the notation used for the key quantities. Unless explicitly stated otherwise, a subscript p indicates a quantity associated with the primary nodes. Similarly, a subscript s, or no subscript, indicates a quantity associated with the secondary nodes. A superscript typically refers to the system or modulation scheme being analyzed.

Table II shows the default values used in our numerical examples. It should be noted that the term $\frac{A\,W}{\pi\, l_p}$ (bits-meter per second) typically has a large value and therefore we use it as our normalization constant. That is, the values of TC shown in our plots are normalized with respect to $\frac{A\,W}{\pi\, l_p}$ (which is equivalent to setting this value to 1 in Table II).

We are now ready to define a general expression for the TC as a function of the secondary nodes' transmission range l_s and their allowed power's pdf $f_P(P)$.

A. Transport Capacity

For a given transmission range (l_s), transmission power (P), and spatial reuse distance (τ), the transport capacity of an OSA MANET over one frequency band $TC_f(l_s, P, \tau)$ can be computed by multiplying the number of simultaneous transmitters ($N_{Active} = \frac{A h_s}{\pi \tau^2}$), the transmission rate R, and the distance traversed by each transmission:

$$TC_f(l_s, P, \tau) \quad = \quad \frac{A h_s R(\gamma) l_s}{\pi \tau^2} \qquad (1)$$

A	:	Network area
W	:	Usable spectrum
M	:	Number of frequency bands
N	:	Number of nodes
N_{Active}	:	Number of nodes transmitting at the same time
σ	:	Density
σ^{Active}	:	Density of nodes transmitting at the same time
α	:	Pathloss exponent
κ	:	Propagation model's constant
η_0	:	Background noise per band
η_p	:	Primary nodes' interference tolerance
I_{Pri}	:	Cumulative interference a primary node experiences due to the transmissions from secondary nodes
I_{Sec}	:	Cumulative interference a secondary node experiences due to the transmissions from secondary nodes
l	:	Transmission range
τ	:	Spatial reuse distance
h	:	Constant relating A, τ, and σ^{Active}
γ	:	Signal-to-Interference-plus-Noise Ratio (SINR)
$R(\gamma)$	:	Modulation-dependent Rate-to-SINR function
θ	:	Target SNR
P	:	Secondary nodes' transmission power
$f_P()$	:	Probability density function of the secondary nodes allowed transmission power
TC_f	:	Per-band Transport Capacity
TC	:	Total Transport Capacity

TABLE I
KEY PARAMETERS AND THEIR NOTATION.

where $R()$ is the rate-to-SINR function determined by the modulation scheme used, and γ is the *Signal to Interference plus Noise Ratio* (SINR), that is,

$$\gamma = \frac{\frac{P}{\kappa l_s^{\alpha}}}{\eta_0 + I_{Sec}} \quad (2)$$

where the numerator corresponds to the transmitter signal's power level at the receiver, η_0 is the background noise over the band f, and I_{Sec} is the cumulative interference of all the other secondary nodes. To compute I_{Sec}, we use the fact that the nodes are uniformly distributed in the area $\mathcal{A}$ and that there are no other transmitters (i.e., interferers) within a radius τ of the receiver (restricted area $\mathcal{R}$). We further assume that the interferers (i.e. the other $N_{Active} - 1$ simultaneous transmitters) are also uniformly distributed outside the restricted area $\mathcal{A} - \mathcal{R}$, with a density $\sigma_s^{Active} = \frac{N_{Active}}{A}$.[5] Therefore, the expected interference can be written as:

$$I_{Sec} = \int_{\mathcal{A}-\mathcal{R}} \frac{P}{\kappa r^{\alpha}} \sigma_s^{Active} \, dA \quad (3)$$

The first element represents the interference induced by any transmitter at a distance r from the receiver, and the second term represents the expected number of such transmitters. By taking into account that for $\alpha > 2$ the values at the boundary of $\mathcal{A}$ become negligible, the above expression can be approximated by extending $\mathcal{A}$ to infinity, resulting in:

$$I_{Sec} \approx \int_{\tau}^{\infty} \frac{P}{\kappa r^{\alpha}} \frac{h_s}{\pi \tau^2} 2\pi r dr = \frac{2h_s}{\alpha - 2} \frac{P}{\kappa \tau^{\alpha}} \quad (4)$$

[5]Strictly speaking, the spatial reuse rules impose a correlation between active nodes location — i.e., they cannot be less than τ meters apart, — however, it is still reasonable to assume that the expected number of *active* nodes in an area A' s.t. $\pi\tau^2 << A' << A$ be $\approx \sigma_s^{Active}$.

α	$\frac{A\,W}{\pi\,l_p}$	$\frac{\eta_p}{\eta_0}$	h_p	h_s	θ_p	θ_s
4	1	1	1	1	16	16

TABLE II
DEFAULT VALUES USED IN THE NUMERICAL EXAMPLES.

that is, the cumulative interference is related to the single-user interference by a constant factor. Replacing (4) in (2) and (1), we obtain:

$$TC_f(l_s, P, \tau) = \frac{Ah_s}{\pi} \frac{l_s}{\tau^2} R\left(\frac{\frac{P}{P_0}(\frac{\tau}{l_s})^{\alpha}}{\frac{2h_s}{\alpha-2}\frac{P}{P_0} + (\frac{\tau}{l_s})^{\alpha}} \right) \quad (5)$$

where $P_0 = \kappa\, l_s^{\alpha}\, \eta_0$ is the transmission power at which the receiver (at a distance l_s) receives the transmitter signal with a power equal to the background noise.

For a given maximum allowed transmission power P, there is an optimal value of τ_{opt} that maximizes $TC_f(l_s, P, \tau)$. The function $TC_f(l_s, P) = TC_f(l_s, P, \tau_{opt})$ is strictly nondecreasing, and can be written as:

$$TC_f(l_s, P) = \frac{Ah_s l_s}{\pi \tau_{opt}^2} R\left(\frac{\frac{P}{P_0}\left(\frac{\tau_{opt}}{l_s}\right)^{\alpha}}{\frac{2h_s}{\alpha-2}\frac{P}{P_0} + \left(\frac{\tau_{opt}}{l_s}\right)^{\alpha}} \right) \quad (6)$$

Now, equation (6) characterize the TC when all the nodes can transmit at the same power. However, in an OSA MANET different nodes have different allowed transmission powers determined by their distance to their closest primary node. To account for these different transmission powers, we use the observation that much of a node's contribution to the total TC is local, through its transmission rate and footprint (spatial reuse area). Thus, we can say that the TC contribution of a node n_i with maximum transmit power P_i over a band f is equal to $\frac{1}{N} TC_f(l_s, P_i)$. Then, adding over all the nodes and all the bands:

$$E\{TC(l_s)\} = E\left\{ \sum_{f_1}^{f_M} \sum_{i=1}^{N} \frac{1}{N} TC_f(l_s, P_i) \right\} = M \int f_P(P)\, TC_f(l_s, P)\, dP \quad (7)$$

where $f_P(.)$ is the pdf of the secondary nodes' *allowed transmission power*.

In the next subsections we describe the modulation schemes studied in this paper (i.e., defining $R(\gamma)$), and provide an expression for $f_P(.)$, which completes our framework.

B. Modulation schemes

In this paper we study the three modulation schemes shown in Figure 1: *Full rate*, *Semilinear*, and *Shannon*.

Under the *Full rate* model, a rate of W/M (i.e., bandwidth efficiency of 1) is achieved *if and only if* the SINR is greater than a threshold value θ, typically between 9–15 dB. That is,

$$R^{Fr}(\gamma) = \begin{cases} 0 & \text{If } \gamma < \theta \\ \frac{W}{M} & \text{If } \gamma \geq \theta \end{cases} \quad (8)$$

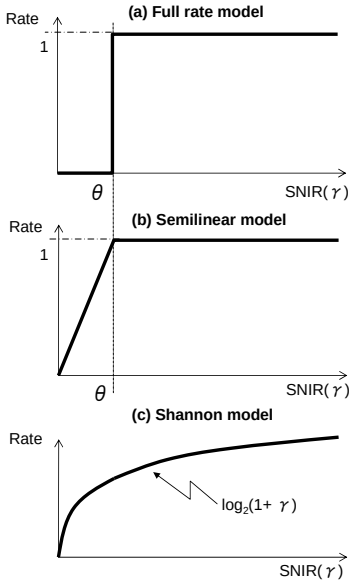

Fig. 1. Transmission rate as a function of the Signal-to-Interference-plus-Noise Ratio (SINR) for the modulation schemes studied in this paper.

Note that the *Full rate* model's discontinuous behavior does not originate from any Bit Error Rate (BER) curve — where the probability of error varies continuously with the SINR — but the discontinuity is due to the design decision of only using those *good* opportunities where the policy-allowed power is strong enough to close the link at the desired rate and error probability.

The *Semilinear* modulation model is an improvement over the *Full rate* model in which opportunities with an allowed transmission power lower than the minimum needed to close the link at full rate are not discarded, but rather exploited — at a lower rate. Its rate-to-SINR function is:

$$R^{Sl}(\gamma) \;=\; \begin{cases} \frac{\gamma}{\theta}\,\frac{W}{M} & \text{If } \gamma < \theta \\ \frac{W}{M} & \text{If } \gamma \geq \theta \end{cases} \qquad (9)$$

An example of a modulation scheme that accomplishes the R^{Sl} function, is the family of Quadrature Phase Shift Keying (QPSK) Direct Sequence Spread Spectrum (DSSS) signals, where different processing gain values result in different points in the "linear" region of R^{Sl}.

The *Semilinear* model has the apparent shortcoming of not exploiting large values of γ to obtain higher transmission rates. To assess the impact of having a bounded transmission rate, we included the *Shannon* model — with its unbounded transmission rate — in our study.

The *Shannon* modulation model represents the maximum rate achieved by a single-user communication system. While no modulation/coding scheme is known to achieve such value, it is theoretically achievable, and therefore it represents the upper bound on the performance of any system. The rate-to-SINR function in this system is the well-known Shannon's capacity formula:

$$R^{Sh}(\gamma) \;=\; \frac{W}{M}\log_2(1+\gamma) \qquad (10)$$

C. OSA allowed transmission power

Under OSA policy, a secondary node can transmit with power P over a band f as long as its distance r to the closest *active*[6] primary node (of the class corresponding to the band f) is large enough so that the interference it induces over the primary node is below η_p.[7] In other words, a secondary node can transmit at power P as long as there are no primary nodes in an *exclusion area* A_{exc} of radius $r_p = \left(\frac{P}{\kappa\eta_p}\right)^{\frac{1}{\alpha}}$.

Let σ_p^{Active} represent the density of *active* primary nodes, which may be much smaller than σ_p, the density of deployed primary nodes. As explained before in our spatial reuse discussion, at any given time at most $\frac{Ah_p}{\pi\tau_p^2}$ primary nodes can be receiving a packet. Since $\tau_p = \theta_p^{\frac{1}{\alpha}} l_p$, it follows that $\sigma_p^{Active} = \frac{h_p}{\pi\, l_p^2\, \theta_p^{\frac{2}{\alpha}}}$, where we are assuming the worst-case scenario, that is, the maximum number of active primary nodes are present. This is equivalent to saying that the primary network is fully deployed (i.e., primary signals are present in every single point). OSA access is still possible due to *underlaying* techniques (see [1] and [15]).

Assuming that the set of active primary nodes are uniformly distributed in the network area, the probability that the maximum allowed transmission power P_m is at least P is equal to the probability that there is no active primary node inside the *exclusion area* A_{exc}. Since for $A_{exc} << A$, the number of nodes inside the area A_{exc} (denoted by $N_p(A_{exc})$) has a Poisson distribution of mean $\sigma_p^{Active} A_{exc}$ then the above probability becomes:

$$\begin{aligned} Pr\{P_m \geq P\} &= Pr\{N_p(A_{exc}) = 0\} && (11)\\ &= e^{-\sigma_p^{Active}\pi r_p^2} && (12)\\ &= e^{-qP^{\frac{2}{\alpha}}} && (13) \end{aligned}$$

where $q = \frac{h_p}{l_p^2\,(\kappa\,\eta_p\,\theta)^{2/\alpha}}$. The pdf of the maximum allowed power $f_P(P)$ is found by taking the derivative of $1 - Pr\{P_m \geq P\}$, which results in:

$$f_P(P) \;=\; \frac{2}{\alpha}\,q\,\frac{e^{-q\,P^{\frac{2}{\alpha}}}}{P^{\frac{\alpha-2}{\alpha}}} \qquad (14)$$

Replacing (14) in (7) completely defines the TC for each modulation scheme.

IV. Infinite density

In this section we study the TC of an OSA MANET when the density of the secondary nodes (σ_s) is assumed to be

[6]OSA nodes can take advantage of silent periods on the primary nodes' MAC. Thus, the fundamental limit is not the presence of a primary node, but the fact that the primary node is active (i.e., receiving) at this instant.

[7]This model addresses the interference due to a single transmitter. However, several transmitters may result in a higher combined interference. As suggested in [15] a margin can be added to account for this. However, this margin depends on the *spatial reuse distance* (τ) of the secondary nodes, and thus the maximum transmission power of a secondary node is tied to the secondary network's choice of spatial reuse distance. For simplicity we ignore this dependence for the time being, but it can be shown — see Section VII in [17], — that this simplification has little effect on the quality of our results.

infinite (unbounded), and therefore there is no limit on how small the spatial reuse distance (τ) can be. Such an analysis is useful to understand the tradeoffs when designing a topology control algorithm. Our study covers the three modulation schemes described in Section III-B. Since the *Shannon* model represents the best possible performance, our coverage of the design space is very comprehensive.

A. Full-rate model

For a given value of P, the optimal spatial reuse distance τ_{opt} is the smallest value of τ such that the SINR is greater or equal to θ. By replacing (2) and (4) in the equation $\gamma = \theta$ and then solving for τ we obtain:

$$\tau_{opt}^{Fr} = \left[\left(\frac{2h_s\theta}{\alpha-2}\right)\left(\frac{P}{P-\theta P_0}\right)\right]^{1/\alpha} l_s \qquad (15)$$

where $P_0 = \kappa l_s^{\alpha}\eta_0$, as before, is the transmission power level that results in the transmitter's signal reaching its destination with a receive power equal to the background noise. τ_{opt}^{Fr} is the optimal value since increasing τ above τ_{opt}^{Fr} reduces the spatial reuse without an increase in the transmission rate, resulting in a lower TC. Similarly, reducing τ below τ_{opt}^{Fr} results in an increase of I_{Sec}, a decrease of the SINR below θ and consequently the transmission rate (and TC) dropping to zero.

It should be noted that τ_{opt}^{Fr} is only defined when $P > \theta P_0$. When $P < \theta P_0$ it is impossible to get a SINR above θ and the TC (as a function of the transmission power) is zero. Replacing the value of τ_{opt}^{Fr} in (6) we obtain

$$TC_f^{FR}(l_s, P) = \frac{K_1}{M\theta^{\frac{2}{\alpha}} l_s}\left(1-\frac{\theta P_0}{P}\right)^{\frac{2}{\alpha}} \qquad (16)$$

where $K_1 = \frac{AWh_s^{\frac{\alpha-2}{\alpha}}}{\pi}\left(\frac{\alpha-2}{2}\right)^{\frac{2}{\alpha}}$. Applying (14) and (16) into (7) we obtain the TC as a function of the transmission range. Figure 2 shows an example of the TC for the parameters shown in Table II. For reference, both the *legacy* system (i.e., no limit in transmission power) and the *Simple* system (i.e., the one used in [15]) are shown. We can see that we have two regions, and that the *Full rate* and *Simple* systems have very similar behavior.

To get a better insight into the *Full rate* system behavior, closed-form expressions for an upper (UB) and a lower bound (LB) are derived, by noticing that

$$\left(\frac{2}{\alpha}\right)^{\frac{2}{\alpha}} U\left(P - \frac{\alpha\,\theta}{\alpha-2}P_0\right) \le \left(1-\frac{\theta P_0}{P}\right)^{\frac{2}{\alpha}} \le U(P-\theta P_0)$$

where U(x) is the step function, i.e., $U(x) = 1$ iff $x > 0$. Replacing $\left(1-\frac{\theta P_0}{P}\right)^{\frac{2}{\alpha}}$ in (16) by the above expressions, we obtain the following lower (LB) and upper (UP) bounds:

$$LB(l_s) = \left(\tfrac{2}{\alpha\,\theta}\right)^{\frac{2}{\alpha}} \tfrac{K_1}{l_s}\, e^{-K_5\left(\frac{l_s}{l_p}\right)^2}$$
$$UB(l_s) = \theta^{-\frac{2}{\alpha}} \tfrac{K_1}{l_s}\, e^{-K_6\left(\frac{l_s}{l_p}\right)^2}$$

where K_1 was defined before, $K_5 = h_p\left(\frac{\alpha}{\alpha-2}\frac{\eta_0}{\eta_p}\frac{\theta}{\theta_p}\right)^{\frac{2}{\alpha}}$ and $K_6 = h_p\left(\frac{\eta_0}{\eta_p}\frac{\theta}{\theta_p}\right)^{\frac{2}{\alpha}}$. From the numerical results we observed that UB is a tight bound for the *Full rate* model, while LB is quite close to the *Simple* model.

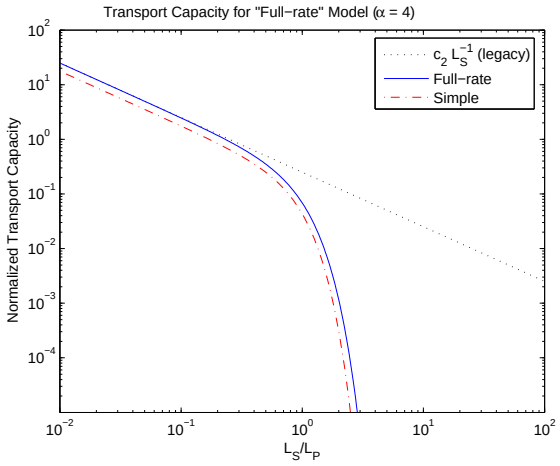

Fig. 2. Transport Capacity versus Transmission Range for the *Full rate* model. There are two operating regions.

We conclude that under the *Full rate* model, TC presents two regions: an *interference limited* region where the system performs similarly to the *legacy* MANETs, and a *policy limited* region where the TC falls steeply when the transmission range is increased. The transition from one region into the other is fast, and around the point where $\frac{l_s}{l_p} = \frac{1}{h_p^{0.5}}\left(\frac{\eta_p}{\eta_0}\frac{\theta_p}{\theta}\right)^{\frac{1}{\alpha}}$.

B. Semilinear model

For a given value of P, the optimal spatial reuse distance τ_{opt} is the minimum value of two quantities, that is :

$$\tau_{opt}^{Sl} = \min\{\tau_1(P), \tau_2(P)\}$$
$$\tau_1(P) = \left[\tfrac{2h_s\theta}{\alpha-2}\tfrac{P}{P-\theta P_0}\right]^{1/\alpha} l_s$$
$$\tau_2(P) = \left(\tfrac{Ph_s}{P_0}\right)^{1/\alpha} l_s$$

Where $\tau_1(P)$ is the value of τ that makes the SINR to be equal to θ. $\tau_2(P)$ is the optimal τ for an auxiliary system obtained by modifying $R^{Sl}(\gamma)$ in Eq.(9), to extend its linear region to infinite, that is, $R^{aux}(\gamma) = \frac{W}{M\theta}\gamma$. Applying R^{aux} in (5) results in a $TC_f^{aux}(l_s, P, \tau)$ function that is *concave down* with respect to τ and has a global maximum at τ_2. τ_2 is easily computed by taking $TC_f^{aux}(l_s, P, \tau)$ first derivative, equating it to zero, and solving for τ.

It can be easily seen that when $\tau > \tau_1(P)$, the SINR region is in the "flat" region of $R^{Sl}(\gamma)$ (see Eq. (9)) and the TC decreases with τ, i.e., $TC(l_s, P, \tau_1(P)) > TC(l_s, P, \tau)$ for every $\tau > \tau_1(P)$. When $\tau \in [0, \tau_1(P)]$, the SINR is in the linear region of $R^{Sl}(\gamma)$, and the TC of the *Semilinear* model is the same as the one from the auxiliary system $TC_f^{aux}(l_s, P, \tau)$, that is, it is *concave down* with a global maximum — if reached — at $\tau_2(P)$. Therefore, if $\tau_2(P) < \tau_1(P)$, the point $TC_f^{Sl}(l_s, P, \tau_2(P)) \ge TC_f^{Sl}(l_s, P, \tau)$ for every $\tau \in [0, \tau_1(P)]$, and in particular $TC_f^{Sl}(l_s, P, \tau_2(P)) \ge TC_f^{Sl}(l_s, P, \tau_1(P))$, and since $TC_f^{Sl}(l_s, P, \tau_1(P)) \ge TC_f^{Sl}(l_s, P, \tau)$ for every $\tau > \tau_1(P)$ we conclude that $TC_f^{Sl}(l_s, P, \tau_2(P))$ is the maximum

value of TC and therefore $\tau_{opt}^{Sl} = \tau_2(P)$. On the other hand, when $\tau_2(P) > \tau_1(P)$, we can see that for $\tau \leq \tau_1(P)$ (the *linear* region) $TC_f^{Sl}(l_s, P, \tau)$ is monotonically increasing and therefore it peaks at the upper limit of the linear region, that is, it peaks at $\tau_1(P)$. Since for $\tau > \tau_1(P)$ (the *flat* region) TC decreases with respect to τ in follows that $TC_f^{Sl}(l_s, P, \tau_1(P))$ is the maximum value of TC and therefore $\tau_{opt}^{Sl} = \tau_1(P)$.

From the above, we have two operation regions, with a transition point at P_2, the point where $\tau_1(P_2) = \tau_2(P_2)$, that is, $P_2 = \frac{\alpha}{\alpha-2}\theta P_0$, where P_0, as defined before, is $P_0 = \kappa l_s^{\alpha}\eta_0$. τ_{opt}^{Sl} is then:

$$\tau_{opt}^{Sl} = \begin{cases} \left(\frac{Ph_s}{P_0}\right)^{\frac{1}{\alpha}} l_s & \text{If } P \leq \frac{\alpha}{\alpha-2}\theta P_0 \\ \left[\left(\frac{2h_s\theta}{\alpha-2}\right)\left(\frac{P}{P-\theta P_0}\right)\right]^{\frac{1}{\alpha}} l_s & \text{If } P > \frac{\alpha}{\alpha-2}\theta P_0 \end{cases} \quad (17)$$

And $TC_f^{Sl}(l_s, P)$ can be written as:

$$TC_f^{Sl}(l_s, P) = \begin{cases} \frac{K_2}{M\,\theta\,l_s}\left(\frac{P}{P_0}\right)^{\frac{\alpha-2}{\alpha}} & \text{If } P \leq \frac{\alpha}{\alpha-2}\theta P_0 \\ \frac{K_1}{M\,\theta^{\frac{2}{\alpha}} l_s}\left(1-\frac{\theta P_0}{P}\right)^{\frac{2}{\alpha}} & \text{If } P > \frac{\alpha}{\alpha-2}\theta P_0 \end{cases} \quad (18)$$

Where K_1 was defined before and $K_2 = \frac{AW}{\pi}\frac{\alpha-2}{\alpha}h_s^{\frac{\alpha-2}{\alpha}}$.

It is interesting to note that for small values of P (i.e., $P < P_2$), the optimal τ_{opt} satisfies $\frac{P}{\kappa\tau_{opt}^{\alpha}} = \frac{\eta_0}{h_s}$, and $I_{Sec} = \frac{2}{\alpha-2}\eta_0$. That is, when P is small, the optimal strategy is to reduce the spatial reuse distance to the point where the interference is constant and thus SINR varies linearly with P (smaller P smaller SINR).[8] The *Full rate* model (previous section) fails to exploit low values of SINR and therefore results in really bad performance for small values of P. For large values of P (i.e., $P > P_2$), τ_{opt} increases slowly, converging to $\left(\frac{2h_s\theta}{\alpha-2}\right)^{\frac{1}{\alpha}} l_s$ as P approaches infinity. Thus, when P is large, the optimal strategy is to keep the spatial reuse distance bounded, let the receive power and interference grow (even to infinity), and have the SINR converge to a constant value.

By replacing (14) and (18) in (7) and after introducing a variable $y = qP^{2/\alpha}$, we found TC^{Sl} to be:

$$TC^{Sl} = \frac{K_2K_7}{\theta^{\frac{2}{\alpha}}l_s}\left(\frac{l_p}{l_s}\right)^{\alpha-2}\int_0^{y_2} y^{\frac{\alpha-2}{2}}e^{-y}dy + \\ + \frac{K_1}{\theta^{\frac{2}{\alpha}}l_s}\int_{y_2}^{+\infty}\left(1-\frac{q^{\frac{\alpha}{2}}P_0}{y^{\frac{\alpha}{2}}}\right)^{\frac{2}{\alpha}}e^{-y}dy \quad (19)$$

where $K_7 = \left(\frac{\eta_p}{\eta_0}\frac{1}{h_p}\right)^{\frac{\alpha-2}{2}}\left(\frac{\theta_p}{\theta}\right)^{\frac{\alpha-2}{\alpha}}$, and $y_2 = \left(\frac{\alpha}{\alpha-2}\frac{\eta_0}{\eta_p}\frac{\theta}{\theta_p}\right)^{2/\alpha}\left(\frac{l_s}{l_p}\right)^2 h_p$.

Eq. (19) can be evaluated numerically. As an example, Figure 3 plots TC^{Sl} computed using the parameters shown earlier in Table II. For reference, the TC of *legacy* MANETs as well as the curve $c_4 l_s^{-3}$ are also shown. It can be seen that under the *Semilinear* model there are still two operating regions and a point of quick transition. For $\frac{l_s}{l_p} << 1$ the system — as before — behaves like a *legacy* MANET with $TC = \Theta\left(\frac{1}{l_s}\right)$. When $\frac{l_s}{l_p} >> 1$ the system transitions to a *policy-limited* region, where TC's rate of decay with respect to l_s is greater (3 in our example and, as it will be shown immediately next, $\alpha - 1$ in general). This significantly differs from the results obtained with the *Full rate* model, where the TC fell steeply with respect to l_s. The reason for the *Full rate* system's poor performance is its inability to exploit situations with small SINR, a technological — rather than fundamental — limitation.

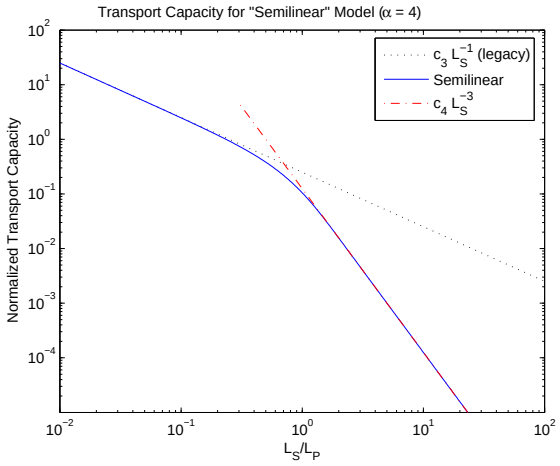

Fig. 3. Transport Capacity versus Transmission Range for the *Semilinear* model. There are two operating regions.

To better understand TC^{Sl} behavior, we derive some closed-form approximations. By looking at the second integral in (19) we notice that $\left(1-\frac{q^{\alpha/2}P_0}{y^{\alpha/2}}\right)^{\frac{2}{\alpha}}$ varies from $(2/\alpha)^{2/\alpha}$ to 1 when y varies from y_2 to $+\infty$. Thus, there exists an $\epsilon_1 \in [\left(\frac{2}{\alpha}\right)^{\frac{2}{\alpha}}, 1]$ such that $\int_{y_2}^{+\infty}\left(1-\frac{q^{\alpha/2}P_0}{y^{\alpha/2}}\right)^{\frac{2}{\alpha}}e^{-y}dy = \epsilon_1\int_{y_2}^{+\infty}e^{-y}dy = \epsilon_1 e^{-y_2}$, and therefore TC^{Sl} can be written as:

$$TC^{Sl} = \frac{K_2K_7}{\theta^{\frac{2}{\alpha}}l_s}\left(\frac{l_p}{l_s}\right)^{\alpha-2}\int_0^{y_2} y^{\frac{\alpha-2}{2}}e^{-y}dy + \frac{K_1\epsilon_1}{\theta^{\frac{2}{\alpha}}}\frac{e^{-y_2}}{l_s} \quad (20)$$

We then consider two cases

1) $\frac{l_s}{l_p} < \left[\frac{\alpha-2}{\alpha}\frac{\eta_p}{\eta_0}\frac{\theta_p}{\theta}\right]^{1/\alpha}\frac{1}{h_p^{1/2}}$*:* In this case y_2 is small. Similar as before, for $y \in [0, y_2]$ we have $e^{-y_2} \leq e^{-y} \leq 1$, and there exists an $\epsilon_2 \in [e^{-y_2}, 1]$ such that $\int_0^{y_2} y^{(\alpha-2)/2}e^{-y}dy = \epsilon_2\int_0^{y_2} y^{(\alpha-2)/2}dy = \frac{2\epsilon_2}{\alpha}y_2^{\alpha/2}$. Replacing in (20) we obtain:

$$TC^{Sl} \approx \left[K_2K_8\epsilon_2\left(\frac{l_s}{l_p}\right)^2 + K_1\epsilon_1 e^{-y_2}\right]\frac{1}{\theta^{\frac{2}{\alpha}}l_s} \quad (21)$$

where $K_8 = \frac{2}{\alpha-2}\left(\frac{\eta_p}{\eta_0}\right)^{\frac{\alpha-4}{2}}\left(\frac{\theta}{\theta_p}\right)^{\frac{2}{\alpha}}h_p$. It can be seen that for small l_s, the term $(\frac{l_s}{l_p})^2$ is small compared with e^{-y_2}

[8]Note that τ_{opt} is, in this regime, also proportional to the carrier sensing range. Also, note that this strategy assumes that τ can be reduced as needed, and there will be secondary nodes close enough to exploit the spatial reuse (unbounded density). In the next section we study the case when the density is bounded.

and the second term dominates equation (21), i.e., $TC^{Sl} \approx \frac{K_1 \epsilon_1 e^{-y_2}}{\theta^{2/\alpha}} \frac{1}{l_s}$, which is $\Theta\left(\frac{1}{l_s}\right)$ for small values of l_s (since y_2 rapidly approaches 0 and e^{-y_2} rapidly approaches 1).

2) $\frac{l_s}{l_p} > \left[\frac{\alpha-2}{\alpha}\frac{\eta_p}{\eta_0}\frac{\theta_p}{\theta}\right]^{\frac{1}{\alpha}} \frac{1}{h_p^{1/2}}$*:* In this case y_2 is large, and we can approximate $\int_0^{y_2} y^{\frac{\alpha-2}{2}} e^{-y} dy \approx \int_0^{+\infty} y^{\frac{\alpha-2}{2}} e^{-y} dy = \Gamma\left(\frac{\alpha}{2}\right)$. Where $\Gamma(x)$ is the well known Gamma function. Also, the term $e^{-y_2} = e^{-K_9\left(\frac{l_s}{l_p}\right)^2}$ vanishes much faster than the others and thus we can write:

$$TC^{Sl} \approx \frac{K_2 K_7 \Gamma\left(\frac{\alpha}{2}\right)}{\theta^{\frac{2}{\alpha}}} \left(\frac{l_p}{l_s}\right)^{\alpha-2} \frac{1}{l_s} \quad (22)$$

And, as we can see, for large l_s, the $TC^{Sl} = \Theta\left(\left(\frac{1}{l_s}\right)^{\alpha-1}\right)$.

C. Shannon Model

$TC_f^{Sh}(l_s, P, \tau)$ can be found by replacing (10) in (5):

$$TC_f^{Sh}(l_s, P, \tau) = \frac{A h_s l_s}{\pi \log(2) \tau^2} \frac{W}{M} log\left(1 + \frac{\frac{P}{P_0}(\frac{\tau}{l_s})^\alpha}{\frac{2h_s}{\alpha-2}\frac{P}{P_0} + (\frac{\tau}{l_s})^\alpha}\right)$$

where $\log(x)$ is the natural logarithm of x.

The optimal value of τ_{opt} is found by setting the derivative of TC_f equal to zero. $\tau_{opt}^{Sh} = l_s\, \tau_*$, where τ_* is the solution to the equation:

$$\frac{b\,\alpha\,\tau_*^\alpha}{[(a+1)\tau_*^\alpha + b][a\tau_*^\alpha + b]} - 2log\left(1 + \frac{\tau_*^\alpha}{a\tau_*^\alpha + b}\right) = 0 \quad (23)$$

where $a = \frac{P_0}{P}$ and $b = \frac{2h_s}{\alpha-2}$. While (23) can be solved numerically, we derive some approximate expressions to gain some insights into the system's behavior.

(i) When $P << P_0$, a is large and $log(1+x) \approx x$. Replacing in (23) we obtain $\tau_* \approx \left[\frac{\alpha-2}{2}\frac{b}{1+a}\right]^{\frac{1}{\alpha}} = \left(\frac{Ph_s}{P+P_0}\right)^{\frac{1}{\alpha}}$.

(ii) When $P >> P_0$, a is small and the terms $a\tau_*^\alpha$ can be ignored, resulting in an equation that does not depend on P. Thus, $\tau_* \approx \left(\frac{2h_s\gamma_\alpha}{\alpha-2}\right)^{\frac{1}{\alpha}}$, where γ_α is the root of the equation $\frac{1+\gamma}{\gamma} log(1+\gamma) = \frac{\alpha}{2}$. It should be noted that γ_α is the optimal SINR when there is no limit in the transmission power, i.e. it is the value the optimal SINR tends to when P grows to infinity, and only depends on α (e.g., $\gamma_{\alpha=4} = 3.9220$).

Combining (i) and (ii), τ_{opt}^{Sh} can be approximated by:

$$\tau_{opt}^{Sh} \approx \begin{cases} \left(\frac{Ph_s}{P+P_0}\right)^{\frac{1}{\alpha}} l_s & \text{If } P << P_0 \\ \left(\frac{2h_s}{\alpha-2} r_\alpha\right)^{\frac{1}{\alpha}} l_s & \text{If } P >> P_0 \end{cases} \quad (24)$$

And, by applying (24) in (6) we obtain:

$$TC_f^{Sh}(l_s, P) \approx \begin{cases} \frac{K_2}{M \log(2) l_s} \left(\frac{P}{P_0}\right)^{\frac{\alpha-2}{\alpha}} & \text{If } P << P_0 \\ \frac{\log(1+r_\alpha)}{r_\alpha^{2/\alpha} M \log(2)} \frac{K_1}{l_s} & \text{If } P >> P_0 \end{cases} \quad (25)$$

Comparing (24)-(25) with (17)-(18) we note a great similarity between the *Semilinear* and *Shannon* systems. Both systems present a similar behavior: when allowed power is small, their spatial reuse distance is reduced, so that the interference remains constant. As power increases, the spatial reuse distance converges to a constant value and even as power approaches infinity, the SINR remains bounded. This was obvious for the *Semilinear* model, whose $R^{Sl}(\gamma)$ presents a flat region (see Figure 1b) above which it makes no sense to increase the SINR, but this is not so obvious for the *Shannon* system, where the $R^{Sh}(\gamma)$ keeps growing to infinity with γ. The reason the *Shannon* system behaves like the *Semilinear* is that $R^{Sh}(\gamma)$ rate of increase for large values of γ is very slow, and therefore it is outweighed by the decrease in spatial reuse needed to increase γ. Thus, *it is not efficient to operate a network at large values of SINR*. It should be noted that the slow slope of $R(\gamma)$ for γ large is a fundamental property of communication systems, based on Shannon's capacity formula, and therefore it is applicable to *any* modulation scheme, not just the ones studied in this paper.

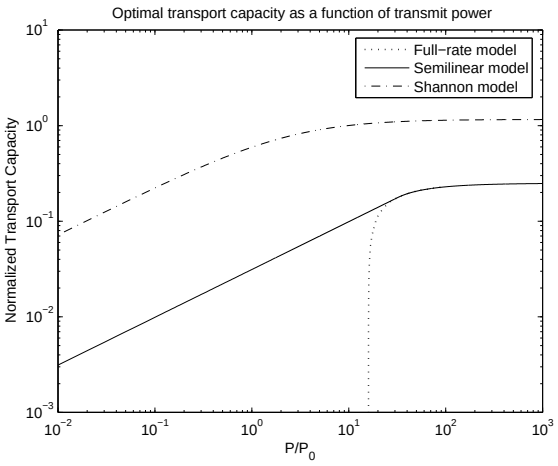

Fig. 4. Transport Capacity versus allowed transmission power for the three modulation schemes. Density is assumed infinite.

To show the similarity between the *Semilinear* and *Shannon* models, Figure 4 plots $TC_f(l_s, P)$ (i.e., TC as a function of P, for a given l_s) for the three modulation schemes considered in this paper. It can be seen that the behaviors of the *Semilinear* and *Shannon* schemes are very similar in both operating regions (low power and high power). Basically they only differ by two constant factors: $f_{lp} = \frac{\theta}{\log 2}$ in the low power region, and $f_{hp} = \left(\frac{\theta}{r_\alpha}\right)^{\frac{2}{\alpha}} \log_2(1 + r_\alpha)$ in the high power region.

Solving (23) and replacing in (7) we can compute $TC^{Sh}(l_s)$, the TC for the *Shannon* system. For example, Figure 5 plots $TC^{Sh}(l_s)$ computed using the parameters shown earlier in Table II (θ is not needed). For reference, the TC of *legacy* MANETs as well as the curve $c_6 l_s^{-3}$ are also shown. As expected from the discussion above, the *Shannon* model behavior is basically the same as the *Semilinear* model's. The slope in the *policy-limited* region is determined by the slope of $TC_f^{Sh}(l_s, P)$ for P small. Since for small values of P both $TC_f^{Sl}(l_s, P)$ and $TC_f^{Sh}(l_s, P)$ have the same slope, then both systems will have the same behavior in the *policy-limited*

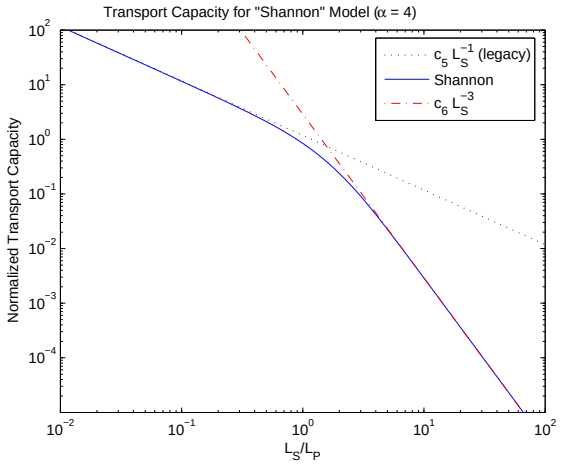

Fig. 5. Transport Capacity versus Transmission Range for the *Shannon* model. There are two operating regions.

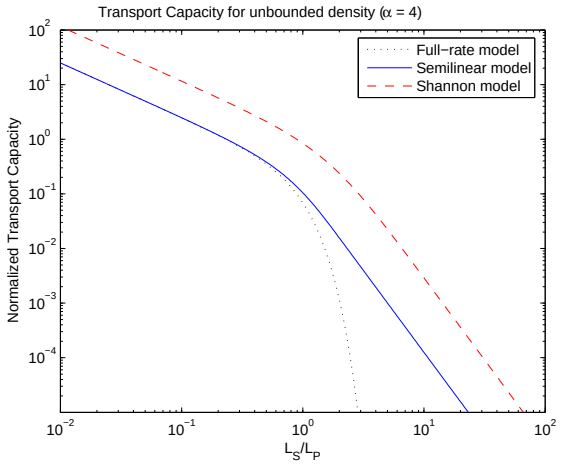

Fig. 6. Transport Capacity versus Transmission Range for the three modulation schemes studied. Density is assumed infinite.

region. That is, when $l_s >> l_p$ then $TC(l_s) = \Theta\left(l_s^{-(\alpha-1)}\right)$.

Finally, Figure 6 summarizes this section's results, comparing $TC(l_s)$ — i.e., TC as a function of the transmission range l_s of the secondary nodes — for the three modulation schemes studied. We can see that while the existence of two operating regions is common to all of them and it is due to a fundamental property of OSA MANETs, the fast decay observed in [15] and the *Full rate* model is not fundamental but due to to shortcomings of that particular modulation scheme. Furthermore, we can see that the *Semilinear* model tracks the *Shannon* model's behavior (within a multiplicative factor). Therefore, without loss of generality, in the remainder of this paper we will focus on the *Semilinear* model — which is more amenable for closed-form solutions, — with the understanding that the results obtained are general.

V. Finite density

In this section, we shift our attention to the *topology design* problem where the control parameter is the finite density (or similarly, the number of the secondary nodes present). We want to determine the impact of the density of the secondary nodes in their TC.

Here we assume that the secondary nodes optimally adjust their transmission range l_s, setting it to the minimum value that keeps the network connected (see [3] and [16]). That is, l_s is set to a value similar to the minimum distance between neighboring nodes. Since there is a one-to-one mapping between the density of the secondary nodes σ_s and this optimal transmission range l_s, and in order to directly apply our framework, we will refer to l_s as our control variable, but it should be kept in mind that l_s is *not* a free variable but it is determined by σ_s.

Since it was already established that both the *Semilinear* and *Shannon* models result in the same asymptotic behavior, we will only focus on the *Semilinear* model in this section. The *Semilinear* model is preferred since it provides easier to understand closed-form expressions, providing better insight.

With this setup, the framework developed in Section III is still valid, with the only difference that the domain of the variable τ (spatial reuse distance) is restricted to the interval $[l_s, +\infty]$, since l_s is the minimum distance between secondary nodes. Thus, equation (17) needs to be modified as follows:

$$\tau_{opt}^{Sl,b} = \begin{cases} l_s & \text{If } P \le \frac{P_0}{h_s} \\ \left(\frac{Ph_s}{P_0}\right)^{\frac{1}{\alpha}} l_s & \text{If } \frac{P_0}{h_s} \le P \le \frac{\alpha}{\alpha-2}\theta P_0 \\ \left[\left(\frac{2h_s\theta}{\alpha-2}\right)\left(\frac{P}{P-\theta P_0}\right)\right]^{\frac{1}{\alpha}} l_s & \text{If } P > \frac{\alpha}{\alpha-2}\theta P_0 \end{cases} \quad (26)$$

Applying (26), $TC(l_s, P)$ is computed as:

$$TC_f^{Sl,b}(l_s, P) = \begin{cases} \frac{AWh_s}{M\pi\theta l_s}\left(\frac{P}{P_0+(\frac{2h_s}{\alpha-2})P}\right) & \text{If } P \le \frac{P_0}{h_s} \\ \frac{K_2}{M\theta l_s}\left(\frac{P}{P_0}\right)^{\frac{\alpha-2}{\alpha}} & \text{If } \frac{P_0}{h_s} < P \le \frac{\alpha}{\alpha-2}\theta P_0 \\ \frac{K_1}{M\theta^{\frac{2}{\alpha}} l_s}\left(1-\frac{\theta P_0}{P}\right)^{\frac{2}{\alpha}} & \text{If } P > \frac{\alpha}{\alpha-2}\theta P_0 \end{cases} \quad (27)$$

By replacing (14) and (27) in (7) we obtain the TC as the sum of three integrals, one for each interval in (27):

$$\begin{aligned} TC^{Sl,b} \;=\; & \frac{K_{10}}{l_s}\int_0^{y_1} \frac{y^{\frac{\alpha}{2}}}{y_1^{\frac{\alpha}{2}} + \frac{2}{\alpha-2}y^{\frac{\alpha}{2}}} e^{-y}dy + \\ & + \frac{K_2K_7}{\theta^{\frac{2}{\alpha}} l_s}\left(\frac{l_p}{l_s}\right)^{\alpha-2}\int_{y_1}^{y_2} y^{\frac{\alpha-2}{2}} e^{-y}dy + \\ & + \frac{K_1}{\theta^{\frac{2}{\alpha}} l_s}\int_{y_2}^{+\infty}\left(1-\frac{q^{\frac{\alpha}{2}}P_0}{y^{\frac{\alpha}{2}}}\right)^{\frac{2}{\alpha}} e^{-y}dy \end{aligned} \quad (28)$$

where $y_1 = K_{12}\left(\frac{l_s}{l_p}\right)^2$, and $K_{12} = h_p\left(\frac{\eta_0}{h_s\theta_p\eta_p}\right)^{\frac{2}{\alpha}}$.

Figure 7 shows the TC as a function of transmission range (i.e., tied to the nodes' density) for the parameters shown in Table II. For comparison, we also plot the TC obtained by a *legacy* node (i.e., no restriction on transmission power) and the curve $c_7 l_s^{-5}$ to which TC converges for large values of l_s (small values of density). It can be seen that once again we

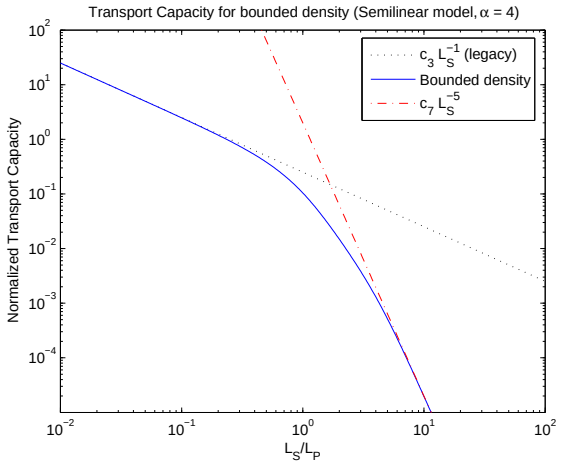

Fig. 7. Transport Capacity versus Transmission Range for the *Semilineal* model. The transmission range is the smallest possible value allowed by the nodes' density.

have two operating regions, with the same transition point. However, TC's rate of decay with l_s is faster than before (unbounded density). As we will see next, for large values of l_s, TC in the bounded-density case is $\Theta\left(\left(\frac{1}{l_s}\right)^{\alpha+1}\right)$.

To understand TC's behavior, we note that when l_s/l_p small, y_1 is small and the last two integrals in (28) dominate the value of $TC^{Sl,b}$. These two integrals are almost identical to the ones in (19) so it is not surprising that for small l_s/l_p we obtain the same behavior as in the unbounded-density case. However, when l_s/l_p is large, y_1 is large, and the first integral dominates $TC^{Sl,b}$ in Eq. (27), and we can write:

$$TC^{Sl,b} \approx \frac{K_{10}}{l_s}\int_0^{y_1}\frac{y^{\frac{\alpha}{2}}}{y_1^{\frac{\alpha}{2}}+\frac{2}{\alpha-2}y^{\frac{\alpha}{2}}}e^{-y}dy \qquad (29)$$

Now, since for $y\in[0,y_1]$

$$\left(\frac{\alpha-2}{\alpha}\right)\frac{1}{y_1^{\frac{\alpha}{2}}} \leq \frac{1}{y_1^{\frac{\alpha}{2}}+\frac{2}{\alpha-2}y^{\frac{\alpha}{2}}} \leq \frac{1}{y_1^{\frac{\alpha}{2}}}$$

then there exists an $\epsilon_3\in[\frac{\alpha-2}{\alpha},1]$ such that

$$TC^{Sl,b} \approx \frac{K_{10}}{l_s}\int_0^{y_1}\epsilon_3\frac{y^{\frac{\alpha}{2}}}{y_1^{\frac{\alpha}{2}}}e^{-y}dy \qquad (30)$$

$$\approx \frac{K_{10}}{l_s}\frac{\epsilon_3}{y_1^{\frac{\alpha}{2}}}\int_0^{+\infty}y^{\frac{\alpha}{2}}e^{-y}dy \qquad (31)$$

$$= \frac{K_{10}}{l_s}\frac{\epsilon_3}{y_1^{\frac{\alpha}{2}}}\Gamma\left(\frac{\alpha}{2}+1\right) \qquad (32)$$

where (31) follows from the fact that since y_1 is a large number, the values of e^{-y} for $y>y_1$ are negligible. Finally, recalling that $y_1=K_{12}\left(\frac{l_s}{l_p}\right)^2$ we obtain that for large values of l_s/l_p, TC is approximately:

$$TC^{Sl,b} \approx \frac{K_{10}\epsilon_3\Gamma\left(\frac{\alpha}{2}+1\right)}{K_{12}^{\frac{\alpha}{2}}}\left(\frac{l_p}{l_s}\right)^{\alpha}\frac{1}{l_s} \qquad (33)$$

that is, for large l_s the TC is $\Theta\left(\left(\frac{1}{l_s}\right)^{\alpha+1}\right)$.

VI. Summary

In this paper we study the TC's dependence on the transmission range for an OSA MANET. We provide an analytical framework and derive closed-form expressions for TC.

Our results show that, regardless of the modulation scheme used, OSA MANETs present two operating regions, depending on the relationship between the transmission range of the primary and secondary nodes (l_p and l_s, respectively). When $l_s < l_p$ the OSA MANET is in the *interference-limited* regime, where TC varies slowly as in *legacy* MANETs, i.e., TC is $\Theta\left(\frac{1}{l_s}\right)$. When $l_s > l_p$, the OSA MANET is in the *policy-limited* regime, where "full-rate" transmissions are not possible, high processing gains are required, and the TC decays faster than expected: $\Theta\left(\left(\frac{1}{l_s}\right)^{\alpha-1}\right)$ if density is unbounded, and $\Theta\left(\left(\frac{1}{l_s}\right)^{\alpha+1}\right)$ if density is bounded, where α is the pathloss exponent.

These results help to understand the behavior of OSA-enabled MANETs, and can guide in the design of a network (e.g., number of nodes needed to cover an area) or developing self-optimizing algorithms (e.g., topology control).

References

[1] A. Zhao and B. M. Sadler, "Dynamic spectrum access: signal processing, networking, and regulatory policy," *To appear in IEEE Signal Processing Magazine*, vol. 24, no. 3, May 2007.

[2] BBN Technologies, "The XG vision, version 2.0," Request For Comment (RFC), accessible at http://www.ir.bbn.com/projects/xmac/vision.html

[3] P. Gupta and P. R. Kumar, "The capacity of wireless networks," *IEEE Trans. in Information Theory*, vol. 46, no. 2, pp. 388–404, Mar. 2000.

[4] A. Jovicic, P. Viswanath, S. R. Kulkarni, "Upper bounds to transport capacity of wireless networks," *IEEE Trans. in Information Theory*, vol. 50, no. 11, pp. 2555–2565, Nov. 2004.

[5] M. Grossglauser, and D. N. C. Tse, "Mobility increases the capacity of ad hoc wireless networks," *IEEE/ACM Trans. on Networking*, vol. 10, no. 4, pp. 477–486, Aug. 2002.

[6] DARPA XG program. http://www.darpa.mil/ato/programs/XG/

[7] M. E. Steenstrup, "Opportunistic use of radio-frequency spectrum: a network perspective," in *Proc. of IEEE DySpan'05*, 2005.

[8] L. Ma, X. Han, and C.C. Shen, "Dynamic open spectrum sharing MAC protocol for wireless ad hoc networks," in *Proc. of IEEE DySpan'05*, 2005.

[9] Q. Zhao, L. Tong, and A. Swami, "Decentralized cognitive mac for dynamic spectrum access," in *Proc. of IEEE DySpan'05*, 2005.

[10] S. Sankaranarayanan et. al., "A bandwidth sharing approach to improve licensed spectrum utilization," in *Proc. of IEEE DySpan'05*, 2005.

[11] S. Seidel, and R. Breinig, "Autonomous dynamic spectrum access system behavior and performance," in *Proc. of IEEE DySPAN'05*, 2005.

[12] J. Zhao, H. Zheng, and G.H. Yang, "Distributed coordination in dynamic spectrum allocation networks," in *Proc. of IEEE DySpan'05*, 2005.

[13] C. Xin, B. Xie, and C.C. Shen, "A novel layered graph model for topology formation and routing in dynamic spectrum access networks," in *Proc. of IEEE DySpan'05*, 2005.

[14] T. Fujii, and Y. Suzuki, "Ad-hoc cognitive radio - development to frequency sharing system by using multi-hop network," in *Proc. of IEEE DySpan'05*, 2005.

[15] C. Santivanez et. al., "XOSA: exploiting opportunistic spectrum access for wireless ad hoc networks," *BBN Technical Report 8410*, BBN Technologies, Cambridge, USA, Dec. 2004.

[16] R. Ramanathan, and R. Rosales-Hain, "Topology control of multihop wireless networks using transmit power adjustment," in *Proc. of IEEE Infocom'00*, 2000.

[17] C. Santivanez, "Transport capacity for opportunistic spectrum access MANETs," *BBN Technical Report 8469*, BBN Technologies, Cambridge, USA, Apr. 2007.